Detecting potential changes in the meridional overturning circulation at 26°N in the Atlantic

Johanna Baehr · Klaus Keller · Jochem Marotzke

Abstract We analyze the ability of an oceanic monitoring array to detect potential changes in the North Atlantic meridional overturning circulation (MOC). The observing array is 'deployed' into a numerical model (ECHAM5/MPI-OM), and simulates the measurements of density and wind stress at 26°N in the Atlantic. The simulated array mimics the continuous monitoring system deployed in the framework of the UK Rapid Climate Change program. We analyze a set of three realizations of a climate change scenario (IPCC A1B), in which – within the considered time-horizon of 200 years – the MOC weakens, but does not collapse. For the detection analysis, we assume that the natural variability of the MOC is known from an independent source, the control run. Our detection approach accounts for the effects of observation errors, infrequent observations, autocorrelated internal variability, and uncertainty in the initial conditions. Continuous observation with the simulated array for approximately 60 years yields a statistically significant ($p < 0.05$) detection with 95 percent reliability assuming a random observation error of 1 Sv (1 Sv $= 10^6$ m^3 s^{-1}). Observing continuously with an observation error of 3 Sv yields a detection time of about 90 years (with 95 percent reliability). Repeated hydrographic transects every 5 years/ 20 years result in a detection time of about 90 years/120 years, with 95 percent reliability and an assumed observation error of 3 Sv. An observation error of 3 Sv (one standard deviation) is a plausible estimate of the observation error associated with the RAPID UK 26°N array.

1 Introduction

Changes in the Atlantic meridional overturning circulation (MOC) are one of the proposed mechanisms associated with past and future abrupt climate change (e.g., Marotzke 2000; National Research Council 2002). Palaeoclimatic records suggest that the ocean circulation

J. Baehr (✉) · J. Marotzke
Max Planck Institute for Meteorology, Bundesstrasse 53, D-20146 Hamburg, Germany
e-mail: johanna.baehr@dkrz.de

K. Keller
Department of Geosciences, The Pennsylvania State University

has undergone rapid changes in the past 120,000 years, since the Eemian interglacial period (Heinrich 1988; Dansgaard et al. 1993; National Research Council 2002; Alley et al. 2003; McManus et al. 2004). Modeling studies have found different responses to anthropogenic climate change, and several model results have suggested that the MOC is potentially sensitive to anthropogenic climate change (e.g., Mikolajewicz and Voss 2000; Thorpe et al. 2001; Gregory et al. 2005). A weakening or collapse of the Atlantic MOC would entail a reduction in the North Atlantic heat transport, which in turn might lead to significant cooling over the North Atlantic and its adjacent regions (Manabe and Stouffer 1994; Vellinga and Wood 2002). The timely detection of MOC changes, and ultimately, timely MOC prediction have the potential to inform the design of climate risk management strategies and decision-making (Keller et al. 2004, 2007).

The MOC is a function of both latitude and depth. In a numerical model the maximum of the MOC across all latitudes is readily derived from the meridional velocity field, but observations yield information only at the latitude of observation. In the Atlantic, the MOC comprises both a (dominating) buoyancy driven contribution, i.e. the thermohaline circulation (THC), and a wind-driven contribution. An observing system is not able to distinguish between these two components, but will be measuring the entire meridional circulation, the MOC.

Observations, commonly hydrographic transects, deliver snapshots of the MOC and the related heat transport at certain latitudes (Hall and Bryden 1982; Ganachaud and Wunsch 2000; Bryden et al. 2005). A strategy to monitor the MOC continuously was suggested by Marotzke et al. (1999), using endpoint measurements of the density at the eastern and western boundary of a zonal transect. Two model-based array design studies (Hirschi et al. 2003; Baehr et al. 2004) suggested that this monitoring array is indeed able to capture both the temporal variability and the mean value of the MOC at 26°N in the Atlantic. These studies focused on the main characteristics of the MOC and its short-term variability. Here, we analyze the proposed MOC monitoring strategy with respect to its capability to detect potential long-term MOC changes at 26°N. The simulated array is kept as close as possible to previous studies. It uses the same observing strategy as Hirschi et al. (2003) and Baehr et al. (2004), and mimics the monitoring system deployed in the framework of the UK Rapid Climate Change program (Marotzke et al. 2002). We restrict our analysis to the 26°N setup, assuming that knowing the MOC at 26°N would provide crucial information about the North Atlantic MOC, its variability and potential changes.

Essentially, we reduce the information delivered by the observing array to a one-dimensional time series to simplify the detection task. This approach expands on the study of Santer et al. (1995), who also reduced the dimensionality of the multivariate problem to a few characteristic integral quantities of the ocean circulation. Banks and Wood (2002) used a numerical model to explore the question of where to look for anthropogenic changes in the ocean. Guided by an optimization of the signal-to-noise ratio, they concluded that the MOC or its associated heat transport are unlikely to be useful for the detection of anthropogenic climate change, since this would require a continuous time series. Similarly, Vellinga and Wood (2004) used an optimal fingerprint based on a maximization of the signal-to-noise ratio to identify locations for potentially useful ocean hydrographic observations, complementing MOC observations at 26°N in the Atlantic. Two dynamical studies (Hu et al. 2004; Latif et al. 2004) used numerical models to identify simple measures allowing to detect changes in the MOC. All these studies employed numerical models to investigate the mechanisms or general nature of detecting changes in the MOC in the Atlantic, but were not directed at realistic observing systems. In contrast, Keller et al. (2006) considered the effects of observation error and infrequent observations, analyzing the required frequency of hydrographic transects in the North Atlantic to detect changes in the MOC. In the present study, we simulate a

realistic observing system, which was deployed recently (Marotzke et al. 2002; Schiermeier 2004). The dynamical background of this observing system has been intensively analyzed (Marotzke et al. 1999; Hirschi et al. 2003; Baehr et al. 2004; Hirschi and Marotzke 2006). We investigate the capability of the observing system to detect changes in the MOC at 26°N. For the detection analysis, one key improvement over previous work is the joint consideration of the effects of observation errors, autocorrelated variability, uncertainty in the model initial conditions, and the reliability of the observing system.

This paper is organized as follows: Section 2 provides the details of the numerical model, data set and method used to simulate the MOC observing array. In Section 3 two different detection approaches and their results are described. Section 4 discusses these results, and conclusions follow in Section 5.

2 Model and method

2.1 Model

We use model output from the ocean component of the coupled ECHAM5/MPI-OM general circulation model (Roeckner et al. 2003; Marsland et al. 2003). This coupled model does not require flux adjustments. In the ocean model, the horizontal discretization is realized on an orthogonal curvilinear C-grid (Marsland et al. 2003). The average horizontal resolution is 1.5°. The vertical discretization is on z-levels with 40 non-equidistant levels.

The coupled model's mean state was described in Jungclaus et al. (2006), using results from an unperturbed control simulation, forced with preindustrial greenhouse gas concentrations. The North Atlantic MOC reaches its maximum of 18.5 Sv (1 Sv = 10^6 m^3 s^{-1}) at about 40°N at 1000 m depth, which is comparable to observations (Macdonald 1998; Ganachaud and Wunsch 2000). The time averaged Atlantic meridional heat transport has its maximum of 1.15 PW near 20°N. This is within the uncertainty range indicated by Trenberth and Solomon (1994), but smaller than the estimates by Ganachaud and Wunsch (2000) and Talley (2003).

2.2 Data

The present analysis is conducted for an unperturbed control simulation and an ensemble of three realizations forced by the the same climate change scenario using the coupled ECHAM5/MPI-OM model. The simulations start from the same spin-up of the model. The control simulation is forced with preindustrial greenhouse gas concentrations, and has a length of 470 years. The climate change experiments are part of a suite of experiments performed for the IPCC Fourth Assessment Report. Starting from different years of the control run, i.e., three different initial conditions, the experiments are all forced with transient greenhouse gas concentrations and aerosol forcing from preindustrial to present day values for the years 1860 to 2000. Subsequently, the IPCC SRES emission scenario A1B (Nakicenovic and Swart 2000) is used to force the model from 2001 to 2100. In the A1B scenario, the CO_2 concentrations rise from 380 ppmv in the year 2001 to 700 ppmv in the year 2100. The simulations are extended for another 100 years with greenhouse gas concentrations fixed at the levels of the year 2100. Note that this forcing scenario assumes considerable reduction in anthropogenic CO_2 emissions after 2100, compared to many estimates of the business-as-usual scenario. The analyzed time series contain 340 years each. The coupled ECHAM5/MPI-OM model shows an increase in global mean temperature of 3.8 K by the year 2100, relative to 1961–1990. The North Atlantic MOC at 30°N weakens for the A1B scenario from 18.5 Sv to about 11 Sv by the year 2100.
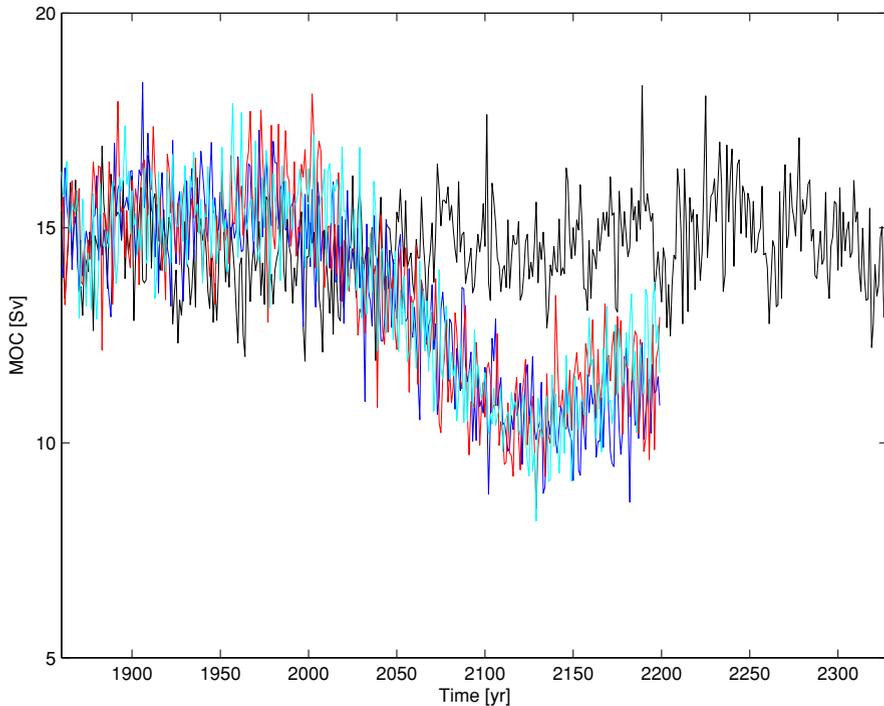
Fig. 1 ECHAM5/MPI-OM MOC time series at 26°N (1000 m), annual mean values; black: control simulation, blue, red, cyan: IPCC scenario A1B. The time axis indicates the years for the forced runs. The time steps of the control run are not associated with realistic years, although the same time axis is used to display the data

At 26°N, the time mean MOC at 1000 m depth is about 15 Sv (Fig. 1). In the forced runs, the MOC weakens to about 11 Sv starting around the year 2000 (Fig. 1), but does not collapse within the considered time-horizon of 200 years. Note that the forcing scenario stabilizes the CO_2 concentrations at 700 ppmv in the year 2100. Many simulations show an MOC collapse beyond the 700 ppmv level (Manabe and Stouffer 1994; Stocker and Schmittner 1997). The simulations analyzed in this study are silent on the question of how the MOC might respond beyond the considered time scale and forcing scenario.

2.3 Simulated MOC measurements

Our conceptual starting point is the thermal wind relationship, which links zonal density differences to the zonally averaged meridional flow. The stream function of a purely buoyancy-driven MOC can be expressed as a function of latitude and density difference between eastern and western sidewalls and other, independent, parameters (Marotzke 1997; Marotzke and Klinger 2000). Marotzke et al. (1999) suggested that, in principle, only the systematic observation of density at eastern and western sidewalls would be required to monitor the MOC continuously. In addition to the thermal wind component, the full MOC comprises a wind-driven component and a depth-independent component (Lee and Marotzke 1997). Concerning the MOC in the North Atlantic, the thermal wind and the Ekman contributions are the dominant contributions (Köhl 2005; Hirschi and Marotzke 2006). These two contributions are measurable; the thermal wind contribution can be derived from the zonal density difference,

and the Ekman contribution can be derived from the surface wind stress. The simulated MOC measurements of Hirschi et al. (2003) and Baehr et al. (2004) employed this decomposition of the MOC, and in addition, the mass balance is closed with a spatially, but not temporally, constant correction (Hall and Bryden 1982).

Similar to Hirschi et al. (2003) and Baehr et al. (2004) we 'deploy' an MOC observing array into a numerical model at 26°N. The placement of density profiles resembles the existing RAPID UK array with dense coverage of the western and eastern boundary (cf. Marotzke et al. 2002). In reality, the meridional transport through the Florida Strait is expected to be measured directly (Larsen 1985, 1992; Baringer and Larsen 2001). However, the model resolution does not allow for a representation of the Florida Strait current and the western boundary current separately. To mimic this additional information we extend the region where the meridional transport is assumed to be known over the complete western boundary region. The knowledge of this transport is updated every three months and random, independent, and normally distributed observation errors with a standard deviation of 1 Sv are added; the level of no motion is placed at the bottom of the zonal section (cf. Hirschi et al. 2003; Baehr et al. 2004).

All simulated observations are assumed to be taken as monthly means, but except where indicated, annual means are formed, and only these are analyzed. The simulated array is capable of reconstructing the low-frequency, as well as the high-frequency, variability of the MOC, in both the control run (Fig. 2a) and the forced runs (Fig. 2b–d). The mean value of
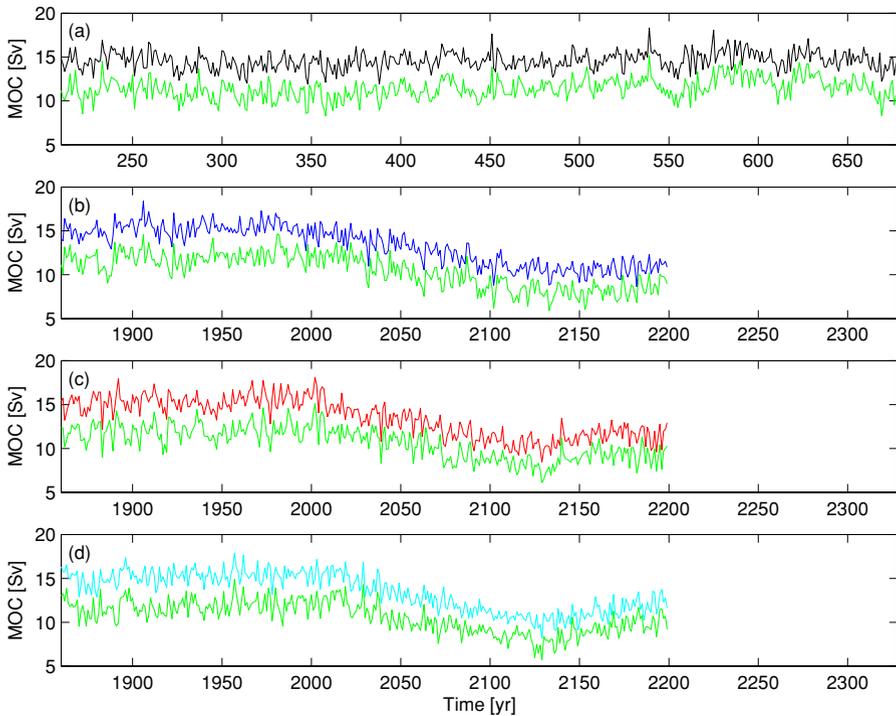

Fig. 2 ECHAM5/MPI-OM MOC time series at 26°N (1000 m), annual mean values; black: model MOC, green: reconstructed MOC based on the simulated 26°N array. (a) control, (b)–(d) three different realizations of the IPCC scenario A1B

the reconstructed MOC is biased by about 4 Sv for both the control run and the forced runs. This offset is nearly constant in time. In the analyzed 340 years it decreases in the forced runs by about 0.5 Sv, whereas no change is apparent in the control simulation.

For the detection analysis, we use normalized time series from which the time mean is subtracted. For the control run, the time mean over the complete 470 years of the time series is subtracted. For the forced run, the time mean over the first 140 years of the time series is subtracted. This approximation seems reasonable, as the detection analysis considers temporal trends, and the temporal variability of the MOC is reconstructed by the array. In reality, occasional hydrographic sections could be used for calibration.

3 Detection analysis

Initially, we use a continuous time series of annual mean values representing the MOC observations at 26°N with no observation error. This time series represents an ideal situation for a detection analysis, as it neglects the effects of infrequent observations and observation error (we relax these simplifying assumptions in Section 3.2.2). The time series are analyzed both qualitatively, employing a simple approach, and quantitatively, employing a more refined statistical approach. The two approaches differ mainly in the way the time series is handled. The simple approach analyzes a series of individual observations, and tests for at each considered time for a potential change. The quantitative approach analyses a sequence of observations and tests for a linear trend. Both methods come to broadly consistent results for the considered case. We discuss both methods to demonstrate that the statistical analysis largely quantifies what is visible by eye. For the quantitative approach, we will further analyze how observation error, shorter time series, and limited observation frequency affect the detection time of MOC changes at 26°N.

3.1 Simple approach

3.1.1 Method

One very simple approach to the detection problem analyses a series of observations, representing an unforced system, and additional independent observations, representing a forced system, and asks whether the forced system is outside the range of natural variability given by the unforced system. The lower and upper bounds characterizing the natural variability of the unforced system, the critical values, can be derived in several different ways. For simplicity, we focus here on three possible definitions of these critical values. Other choices of critical values are possible.

The control run is used to provide the natural variability, i.e., the 'observations' of the unforced system. First (i), the strictest criterion would be to set the critical value to the lowest value 'observed' in the past, given by the natural range of variability. Second (ii), a milder criterion would be to assume that anything lower/higher than two standard deviations of the values 'observed' in the past is critical. Third (iii), we assume that anything lower/higher than the lowest/highest 2.5 percent of the values 'observed' in the past is critical. If the considered time series were independent draws from a single normal distribution, the critical values (ii) and (iii) would be virtually identical. Both would approximate the lower and upper bounds of the 95 percent confidence interval of the underlying distribution of the unforced time series. The control run, however, violates the assumption of independent draws, we will return to this issue below.

3.1.2 Results

For this simple detection approach, the control simulation is used to provide an indication of the natural range of variability of the MOC. The critical values discussed above are derived for both the unforced model MOC and the unforced reconstructed MOC from the simulated array (Fig. 3). The times at which the respective forced run (shown for one realization only) leaves the lower bound of the given range of natural variability, i.e., detection times, are indicated by the dots above the abscissa in Fig. 3. For the model MOC, detection occurs around the year 2030 for the critical values (ii) and (iii), whereas for the critical value (i) detection occurs around the year 2060 (Fig. 3a). Detection prior to the year 2030 is predominantly the result of type-I errors in statistical hypothesis testing, i.e., falsely rejecting the null hypothesis of no change. Adopting the typically used *p*-value of 0.05 implies a type-I error frequency of 5 percent. More specifically, allowing 5 percent of the values to be outside the critical values results in 5 percent false alarms.

For the reconstructed MOC from the simulated array, detection for the critical value (i) occurs around year 2060 (Fig. 3b), as for the model MOC. For the moderate critical values (ii) and (iii), detection occurs around year 2035 (Fig. 3a), which is somewhat later than for the model MOC. The same is found for the two other realizations of the forced run (not
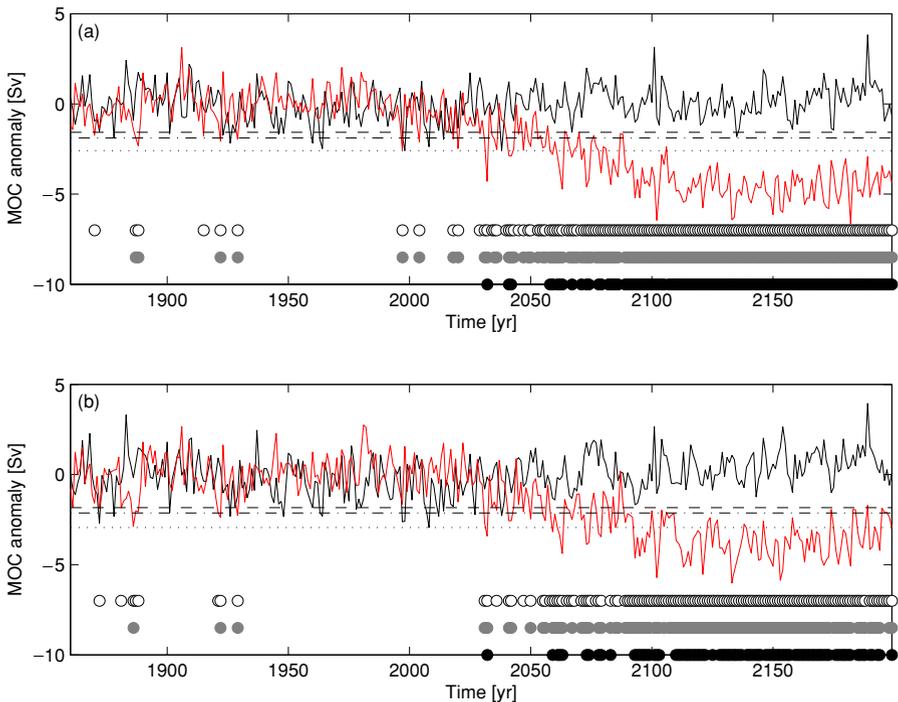

Fig. 3 MOC time series at 26°N at 1000 m, annual mean values. The horizontal lines indicate different critical values, each derived from the variability of the control time series (see text for details). Dots indicate times at which the forced MOC falls below the respective critical value. Three different critical values are shown: (I) minimum of the control time series (dotted line, black dots), (II) lower bound 95 percent confidence level (dash-dotted line, grey dots), (III) the lowest/highest 2.5 percent of the values of the entire control time series (dashed line, open circle). (a) ECHAM5/MPI-OM, (b) Array reconstruction

shown). The times at which the model MOC and the reconstructed MOC from the simulated array fall below the respective critical value are similar, but in some cases detection occurs for the simulated array up to 10 years later than for the model MOC.

To summarize, the detection times derived from the model MOC and the reconstructed MOC from the simulated array are similar. However, this qualitative analysis does not allow us to make formal statistical statements about the detection capability.

3.2 Quantitative approach

3.2.1 Method

We now derive a detection approach that allows us to quantify the detection time of a specific observing system, and therefore allows us to characterize the relationships between detection time, observation error, observation frequency, and the length of observations. First, we use the control simulation to estimate the natural variability of the MOC at 26°N. Second, we test when the forced simulation leaves this range of natural variability.

To estimate the natural variability of the MOC at 26°N, the control run is randomly sampled for a specific length of observation period. Similar to the approach of Santer et al. (1995), the linear trend is estimated for each of these lengths of observation periods, using least squares linear trend estimates. We use overlapping lengths of observation periods with random starting points. We use 10^4 samples for every length of observation period, to yield a numerically stable estimate of the linear trends in the control run. For a given length of observation period, the pdf (probability density function) derived from the linear trends represents the variability of the unforced system. We expand on the method of Santer et al. (1995) by repeating this procedure for a variety of lengths of observation periods, which yields the upper and lower confidence limits of the natural variability, depending on the length of the simulated observations (Fig. 4). To analyze when the forced simulation leaves the range of natural variability, we estimate the linear trend of the forced simulation, starting in year 2005. Using a single realization of the forced simulation, the linear trends depend only on the length of the simulated observations (Fig. 4, solid line).

Detection time is a random variable as it depends on random realizations of the observation errors and the internal variability (Keller et al. 2006). To account for observation error, we add random observation error (identically, independently and normally distributed) of different magnitudes (e.g., standard deviation of 1 Sv) to the simulated observations, and estimate the linear trend of each of the resulting time series. Here, random observation errors are added 10^4 times to the time series, to yield numerically stable results. We add random observation error to both the unforced and the forced time series, assuming that the two time series are observations with an inherent observation error, derived from different sources. For simplicity, we assume the same magnitude of observation error for the unforced and forced time series.

For the unforced time series, the upper bound confidence limit derived from analyzing the tail area of the pdf of the linear trends, yields the estimate of the natural variability (depending on the length of observation period and observation error). For the forced time series, the linear trends are compared to these confidence limits derived from the unforced run (for the respective length of observation period and observation error): the times at which the linear trend of the forced time series with added observation error is outside the confidence limits provided by the unforced time series yield an empirical cdf (cumulative distribution function) over a range of lengths of the observation periods, depending on the observation error (Fig. 5). The upper bound confidence limit derived from analyzing the tail area of this empirical cdf yields the length of observation period at which the forced simulation has left
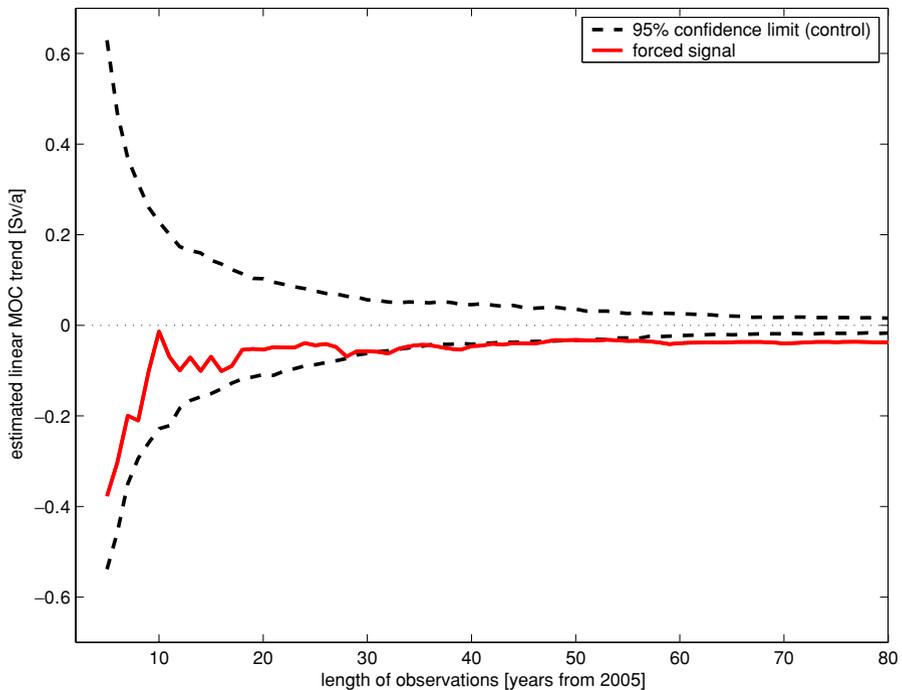
Fig. 4 Upper and lower 95 percent confidence limit of the linear trends derived from bootstrap analysis of the control run (dashed line; random starting points), and one realization of the forced run (red line; starting at the year 2005). Both time series are annual means with no added observation error. The arrow denotes the time at which the statistically significant trend in the forced run is first detected

the range of natural variability with $p < 0.05$ (Table 1). Following Santer et al. (1995), we refer to this time as the 'detection time'. Note that the median detection time, i.e., detecting with a 50 percent reliability (Table 1), is considerably lower than the estimated detection time based on the upper bound 95 percent confidence limit.

Applying this detection method to the control simulation itself, yields a detection frequency of approximately 5 percent. This recovers the value that was used to design the approach, i.e., the type-I error frequency.

3.2.2 Results

3.2.2.1 MOC. Analyzing the forced simulation of the model MOC for an observation error of 1 Sv results in detection times with 95 percent reliability between ∼40 and ∼60 years, depending on the realization (Fig. 5 a,c and Table 1). The median detection time for the equivalent systems is about 30 years smaller than the detection time derived from the upper 95 percent confidence limit (Table 1). An increase in the observation error to 3 Sv results in increased detection times of about ∼80 to ∼100 years (95 percent reliability), and between ∼30 and ∼50 years (50 percent reliability). An analysis of the reconstructed MOC time series from the simulated array yields similar results: detection with 95 percent reliability for an observation error of 1 Sv yields detection times of about ∼50 to ∼70 years, and for an observation error of 3 Sv yields detection times of about ∼90 to ∼100 years
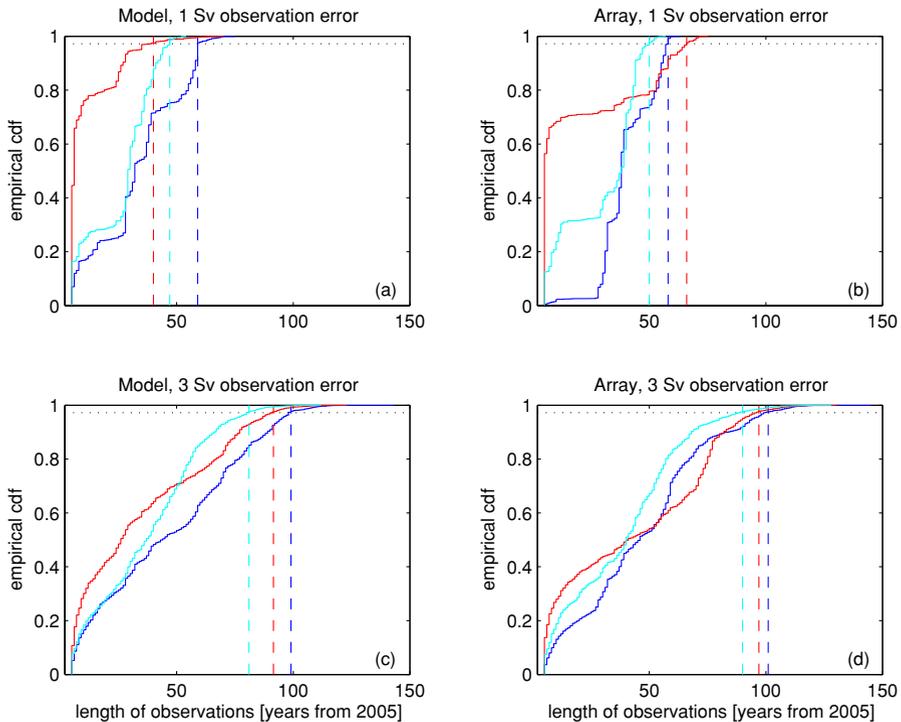
Fig. 5 Empirical cumulative distribution function (cdf; that is, the cumulative sum of the probability density function) of the detection times for different observing systems. The three realizations of the forced run are indicated by the different colors. Dashed lines indicate upper 95 percent confidence limit of the detection time. (a) model, observation error 1 Sv, (b) simulated array, observation error 1 Sv, (c) model, observation error 3 Sv, (d) simulated array, observation error 3 Sv

(Fig. 5 b,d). Larger observation errors of 6 and 8 Sv increase the detection times (with 95 percent reliability) for both the model MOC and the reconstructed MOC from the simulated array to about 135 years (Table 1).

The median detection times for small observation errors derived from the quantitative analysis are similar to the detection times derived for the simple analysis (cf. Fig. 3). These median detection times are furthermore comparable to the time at which a single realization assuming no observation error leaves the range of natural variability for the first time (at about 30 years of simulated observations, cf. Fig. 4). In addition, the detection times derived from the upper 95 percent confidence limit using the quantitative method for small observation errors are similar to the detection time when the single realization assuming no observation error shows a sustained leave of the range of natural variability (at about 60 years of simulated observations, cf. Fig. 4). The results of the two detection approaches differ, because the simple detection approach considers the observations in isolation, whereas the quantitative approach analyses a trend in a sequence of observations.

Previous analysis typically considered a single realization of a model run (e.g., Santer et al. 1995; Vellinga and Wood 2004; Keller et al. 2006). Analyzing a single realization neglects the uncertainty due to the initial conditions. As shown in Fig. 5 and Table 1, the effects of

Table 1 Detection times for continuous observations from the model MOC and reconstructed MOC from the simulated array and as a function of the reliability of the detection system. The three numbers represent the three realizations of the forced run

Observation error	1 Sv	3 Sv	6 Sv	8 Sv
Median detection time (50 percent reliability)				
Model	34, 10, 27	47, 34, 37	56, 50, 50	53, 52, 50
Simulated array	41, 19, 30	47, 43, 39	54, 51, 53	52, 51, 52
Upper 95 percent confidence limit detection time (95 percent reliability)				
Model	59, 40, 47	99, 92, 81	136, 124, 128	142, 135, 135
Simulated array	58, 66, 50	101, 97, 90	136, 130, 130	141, 137, 137

different initial conditions on the detection time can be noticeable, on the order of a decade in our example.

4.2.2.2 Infrequent MOC observations. So far, we only consider continuous observations, using a complete time series of annual mean values. Now, we analyze how lowering the observation frequency would influence the detection time. The time series of monthly means is subsampled at fixed intervals in years, but the month of the specific year is randomly chosen each time; the resulting time series is analyzed in the same way as the time series based on continuous observations. To mimic hydrographic transects accurately, we use the time series of monthly mean values of the MOC of which the short-term, i.e. monthly, variability of the wind-driven circulation is subtracted, but the annual mean of the wind-driven part is kept. The monthly mean MOC at 26°N in ECHAM5/MPI-OM model shows a peak to peak variability of 16 Sv, of which about 6 Sv are purely wind-driven. Subtracting the short-term wind-driven variability is in accordance with procedures analyzing observations, where hydrographic transects are combined with annual mean values of the wind field (e.g., Bryden et al. 2005).

A reduction from continuous observations to frequent hydrographic transects every year or every two years has little effect on the detection time (Table 2). Depending on the realization, the detection time increases or decreases by up to about 5 years. One reason for the decrease in detection time is the failure to properly resolve the high-frequency variability with infrequent observations. Reducing the frequency of observations to 10 or 20 years, a frequency which would arguably be feasible with hydrographic observations, yields considerably longer detection times (Table 2). Observing with an observation error of 3 Sv every 20 years nearly doubles the detection time compared to continuous observations to about 120 years. Two factors influence this increase in detection time. First, the sparse resolution of the time series derived from infrequent sampling is too coarse to yield accurate MOC

Table 2 Detection time (95 percent upper confidence limit) for model MOC, using infrequent observations. The three numbers represent the three realizations of the forced run

| Observation frequency | Observation error | | | |
	1 Sv	3 Sv	6 Sv	8 Sv
Continuous	59, 40, 47	99, 92, 81	136, 124, 128	142, 135, 135
Every yr	63, 39, 43	95, 87, 76	131, 119, 126	139, 133, 135
Every 2 yrs	61, 35, 43	93, 83, 77	119, 113, 115	129, 123, 125
Every 5 yrs	61, 61, 66	91, 86, 86	106, 101, 101	111, 106, 106
Every 10 yrs	81, 71, 71	91, 91, 91	101, 101, 101	101, 111, 111
Every 20 yrs	81, 81, 101	121, 101, 121	121, 121, 121	121, 121, 121

trend estimates. Second, the annual cycle of the density-driven part of the MOC changes, but hydrographic transects neither resolve the annual cycle of the density-driven part of the MOC nor capture its change. These detection times are even larger when observation errors of 6 Sv or 8 Sv are assumed (Table 2): about 120 years assuming a hydrographic transect every 20 years. The estimated detection for the three considered scenarios are not a monotonically increasing function of decreasing observation frequency (Table 2). This is not unexpected, due to the stochastic nature of the problem. Observation frequencies of 1 or 2 years are dominated by the short-term variability, whereas observation frequencies like 10 or 20 years capture mainly the long-term trend. Note that this detection analysis assumes a known natural variability, and a start of the simulated observations close to the begin of an MOC weakening. Both assumptions are not necessarily valid for real MOC observing systems.

4.2.2.3 Meridional heat transport. The velocity field derived from the 26°N monitoring array is capable of delivering information beyond a MOC time series. The meridional heat transport is arguably one of the key quantities of interest, as the MOC carries most of the oceanic heat transport in the Atlantic (Hall and Bryden 1982; Ganachaud and Wunsch 2000). The effect of this northward heat transport of about 1 PW ($=10^{15}$ W; Ganachaud and Wunsch 2000) is seen in the resulting relatively mild climate of Western Europe.

The meridional heat transport can be measured, if in addition to the array, a hydrographic transect is undertaken to measure the temperature field. The additional hydrographic transect is necessary to ensure improved spatial coverage of the small scale structure in the temperature field, providing a reliable heat content estimate. Here, we keep the initially 'measured' temperature field constant until new 'observations' are provided, since short term changes in the meridional heat transport are governed by fluctuations in the velocity field rather than the temperature field (Jayne and Marotzke 2001). Assuming a hydrographic transect every 5 years, and accounting for an observation error of 0.2 PW (cf. Ganachaud and Wunsch 2000) results in a detection time of about 120 years for both the original model heat transport as well as the heat transport derived from the simulated array at 26°N. Lower frequencies of the hydrographic transects (e.g., 10 or 20 years) do not notably increase this detection time in ECHAM5/MPI-OM. However, this insensitivity of the detection time on the frequency of temperature section should be interpreted with caution, since it is likely dependent on the employed model, and its respective resolution. Higher observation errors, up to about 0.5 PW, delay the detection by up to 10 years. The notably larger detection times for the heat transport compared to the MOC arise from the additional influence of the variability in the temperature field combined with the strong internal variability of the ECHAM5/MPI-OM control simulation. Note that this affects the detection time of both the reconstructed heat transport from the simulated array and the model heat transport similarly.

4 Discussion

In the present study, we test whether a time series derived from simulated measurements of the MOC at 26°N is capable of detecting changes in the MOC. Currently, the detection of MOC changes is based on a very limited amount of information: e.g., snapshots of the MOC at certain latitudes (e.g., Bryden et al. 1996, 2003, 2005), results from data assimilation for about a decade (e.g., Stammer et al. 2003; Wunsch and Heimbach 2006), or hindcats estimates (e.g., Marsh et al. 2005). However, a statistically rigorous method would have to be based on more information than is available from current observing systems, since robust detection depends on the additional knowledge of the natural variability of the system

(e.g., Santer et al. 1995). This challenge is inherent to all climate change detection studies, and a refined analysis of the historic observations of the MOC at 26°N (Longworth et al. 2005), or more generally the palaeo-record (e.g., Keigwin and Boyle 2000), might be a promising step towards this goal (Keller et al. 2007).

In our analysis, we estimate the detection time for a range of observation errors. It is difficult to assess, which of these chosen observation errors would be a reasonable approximation to real observations. Ganachaud (2003) estimated the observation error for integrated transports derived from hydrographic transects as approximately 3 Sv (one standard deviation), similar to the error assumed here. Ganachaud (2003) attributed this error mainly to uncertainties due to unknown temporal variability. The observation error of MOC estimates based on the RAPID UK 26°N array is not yet known. The temporal resolution of the array data should, however, allow us to reduce the uncertainties due to the unknown temporal variability of the MOC. A careful assessment of errors in the observed MOC (and associated properties) is crucial for the tasks of MOC change detection, prediction, and the design of observation systems.

An inherent limitation to the transferability of our results is the dependence on the particular model employed. In ECHAM5/MPI-OM, the annual mean MOC at 26°N exhibits a variability from peak to peak of about 4 Sv. This is comparable to results given by other coupled models (Gregory et al. 2005). We use three realizations and find that the results are robust across these three realizations. The actual variability of the MOC is, at this time, uncertain due to the sparse spatiotemporal nature of the available observations.

We have tested our approach with monthly values instead of annual means. Note that in the ECHAM5/MPI-OM model the MOC without short-term wind-driven variability exhibits a peak to peak variability of about 10 Sv arising from fluctuations in the density field. This results in a small signal-to-noise ratio, especially in combination with the weak decline in the ECHAM5/MPI-OM solution. If unsmoothed monthly mean data are used, no detection occurs within the considered time horizon of 200 years, for either the model MOC or the reconstructed MOC from the simulated array (results not shown). Evidently, this changes considerably if the monthly mean time series is smoothed or averaged. However, both techniques require a continuous time series, with a high temporal resolution.

The array simulated in the present study assumes continuous observations. Similar to Keller et al. (2006) we also analyze how less frequent hydrographic sections influence the detection time. Keller et al. (2006) found that an observing system consisting of a hydrographic transect every 5 years and an observation error of about 3 Sv results in a median detection time of approximately 70 years. Our results are broadly consistent with the findings of Keller et al. (2006), who use a different model run (Manabe and Stouffer 1994) and a different statistical detection method. For an observation error of 3 Sv, the median detection time of continuous or infrequent observations (up to observing every 10 years) is within a century in our analysis. But we find, in addition, that observing continuously with an observation error of 1 Sv reduces the 95 percent reliability detection time considerably, in our model to about 40 to 60 years.

The analysis, so far, indicates that establishing a continuous MOC observing system at 26°N lasting for decades has the potential to reduce the currently large uncertainty about the MOC response to anthropogenic forcing. One might ask whether the necessary investments would pass an economic cost-benefit test, as hypothesized by Adams et al. (2000). Previous economic analysis showed that reducing key uncertainties about the impacts of anthropogenic greenhouse gas emissions may allow for economically more efficient strategies of climate risk management and have hence the potential for a positive expected economic value of information (Yohe 1991, 1996; Peck and Teisberg 1996; Nordhaus and Popp 1997; Keller

et al. 2006). Keller et al. (2006) showed that the expected economic value of information of an MOC observing system that would deliver an actionable early warning sign of MOC changes within the next few decades can far exceed the necessary costs.

It is important to recognize, however, that estimates of the economic value of information are an area of active research and hinge on a range of simplifying assumptions. Keller et al. (2006), for example, approximated the decision problem as a binary system. Specifically, the MOC is either insensitive to anthropogenic forcing or sensitive. In addition, the decision-maker chooses between two options: no control of CO_2 emissions or reducing CO_2 emissions such that an MOC collapse is avoided in the sensitive case. In this situation, detecting an MOC change is equivalent to predicting the binary MOC response. In addition, Keller et al. (2006) adopted a simple decision-criterion (expected cost-minimization) and published estimates of the economic impacts of MOC collapse. These assumptions may be reasonable first-order descriptions of the decision-making process, but ignore the effects of (i) structural model uncertainty, (ii) a more refined sampling of the parametric uncertainty, and (iii) alternative decision criteria (Lempert 2002).

Given these caveats, the investments into a decadal-scale and continuous MOC observation array at 26°N has the potential to pass a very simple economic cost-benefit test: the costs of the array are on the scale of 1 million US dollars per year and tens of millions over decades, compared to an expected economic value of information on the order of billions US dollars. The 26°N array has smaller costs than the ones considered in Keller et al. (2006). In addition, the 26°N array provides MOC observations with higher temporal resolution and higher expected accuracy than hydrographic sections, the observing system analyzed in Keller et al. (2006).

The observations provided by the RAPID UK 26°N array deliver a two dimensional picture of the zonal transect at 26°N, which contains more information than just a one-dimensional time series. Applying multivariate fingerprint analysis (Santer et al. 1995; Hasselmann 1998) has the potential to result in shorter detection times. The focus of the present study is to demonstrate, as a first step, the ability of the 26°N array to detect changes in a single time series, the MOC at 26°N, if the unforced variability is known. A multivariate analysis is left for future study.

5 Conclusions

Based on our analysis of a simulated MOC observing array in the particular solutions of ECHAM5/MPI-OM, and our univariate analysis assuming, most notably, that we have independent knowledge of the variability of the unforced system, we conclude:

1. Observation periods of less than 20 years carry a high probability to result in false alarms, i.e., detection times similar to the type-I error frequency used in designing the method.
2. Detecting MOC changes at 26°N with a reliability of 95 percent requires decades to a century of continuous observations, depending on the observation error.
3. For an observation error of 1 Sv, continuous observations result in a detection time of approximately 60 years (with 95 percent reliability). For an observation error of 6 Sv, the 95 percent reliability detection time exceeds a century.
4. Continuous observations, hydrographic sections every 5 years, and hydrographic sections every 20 years result in detection times of about 100 years, 90 years, and 120 years, respectively, for an observation error of 3 Sv, and for a 95 percent reliability.

5. Changes in the meridional heat transport at 26°N can be detected with a detection time of about 120 years (95 percent reliability), assuming an observation error of about 0.2 PW, and additionally assuming a hydrographic transect every 5 years.

6. For a given desired reliability in detecting MOC changes at 26°N, a continuous observing system is less expensive than repeat hydrographic sections.

References

Adams R, Brown M, Colgan C, Flemming N, Kite-Powell H, McCarl B, Mjelde J, Solow A, Teisberg T, Weiher R (2000) The economics of sustained ocean observations: benefits and rationale for public funding. Technical report, A joint publication of the National Oceanic and Atmospheric Administration and the Office of Naval Research

Alley RB, Marotzke J, Nordhaus WD, Overpeck JT, Peteet DM, Pielke Jr. RA, Pierrehumbert RT, Rhines PB, Stocker TF, Talley LD, Wallace JM (2003) Abrupt climate change. Science 299:2005–2010

Baehr J, Hirschi J, Beismann J, Marotzke J (2004) Monitoring the meridional overturning circulation in the North Atlantic: a model-based array design study. Journal of Marine Research 62(3):283–312

Banks H, Wood RA (2002) Where to look for anthropogenic climate change in the ocean? Journal of Climate 15:879–891

Baringer MO, Larsen JC (2001) Sixteen years of Florida current transport at 27°N. Geophysical Research Letters 28:3179–3182

Bryden HL, Griffiths MJ, Lavin AM, Millard RC, Parrilla G, Smethie WM (1996) Decadal changes in water mass characteristics at 24°N in the subtropical North Atlantic. Journal of Climate 9:3162–3186

Bryden HL, Longworth HR, Cunningham SA (2005) Slowing of the Atlantic meridional overturning circulation at 25°N. Nature 438:655–657

Bryden HL, McDonagh EL, King BA (2003) Changes in ocean water mass properties: oscillations or trends? Science 300: 2086–2088

Dansgaard W, Johnsen SJ, Clausen HB, Dahl-Jensen D, Gundestrup NS, Hammer CU, Hvidberg CS, Steffensen JP, Sveinbjoernsdottir AE, Jouzel J, Bond G (1993) Evidence for general instability of past climate from a 250-kyr ice-core record. Nature 364:218–220

Ganachaud A (2003) Error budget of inverse box models: the North Atlantic. Journal of Atmospheric and Oceanic Technology 20:1641–1655

Ganachaud A, Wunsch C (2000) Improved estimates of global ocean circulation, heat transport and mixing from hydrographic data. Nature 408:453–457

Gregory JM, Dixon KW, Stouffer RJ, Weaver AJ, Driesschaert E, Eby M, Fichefet T, Hasumi H, Hu A, Jungclaus JH, Kamenkovich IV, Levermann A, Montoya M, Murakami S, Nawrath S, Oka A, Sokolov AP, Thorpe RB (2005) A model intercomparison of changes in the Atlantic thermohaline circulation in response to increasing atmospheric CO_2 concentration. Geophysical Research Letters 32:L12703, doi: 10.1029/2005GL023209

Hall MM, Bryden HL (1982) Direct estimates and mechanisms of ocean heat transport. Deep Sea Research 29:No. 3A, 339–359

Hasselmann K (1998) Conventional and Bayesian approach to climate-change detection and attribution. Quarterly Journal of the Royal Meteorological Society 124(552):2541–2565

Heinrich H (1988) Origin and consequences of cyclic ice rafting in the Northeast Atlantic Ocean during the past 130,000 years. Quaternary Research 29 (2):142–152

Hirschi J, Baehr J, Marotzke J, Stark J, Cunningham S, Beismann JO (2003) A monitoring design for the Atlantic meridional overturning circulation. Geophysical Research Letters 30(7): 1413, doi: 10.1029/2002GL016776

Hirschi J, Marotzke J (2006) Reconstructing the meridional overturning circulation from boundary densities and zonal wind stress. Submitted to Journal of Physical Oceanography

Hu A, Meehl GA, Han W (2004) Detecting thermohaline circulation changes from ocean properties in a coupled model. Geophysical Research Letters 31: L13204, doi: 10.1029/2004GL020218

Jayne SR, Marotzke J (2001) The dynamics of ocean heat transport variability. Reviews of Geophysics 39:385–411

Jungclaus JH, Botzet M, Haak H, Luo J, Latif M, Marotzke J, Mikolajewicz U, Roeckner E (2006) Ocean circulation and tropical variability in the coupled model ECHAM/MPI-OM. Journal of Climate, Accepted

Keigwin LD, Boyle EA (2000) Detecting Holocene changes in thermohaline circulation. Proceedings of the National Academy of Sciences of the United States of America 97(4):1343–1346

Keller K, Bolker BM, Bradford DF (2004) Uncertain climate thresholds and optimal economic growth. Journal of Environmental Economics and Management 48:723–741

Keller K, Deutsch C, Hall MG, Bradford DF (2006) Early detection of changes in the North Atlantic meridional overturning circulation: implications for the design of ocean observation systems. Journal of Climate, in the press

Keller K, Yohe G, Schlesinger M (2007) Managing the risks of climate thresholds: uncertainties and information needs. Climatic Change, DOI 10.1007/s10584-006-9114-6, this issue

Köhl A (2005) Anomalies of meridional overturning: mechanisms in the North Atlantic. Journal of Physical Oceanography 35:1455–1472

Larsen JC (1985) Florida Current volume transports from voltage measurements. Science 277:302–304

Larsen JC (1992) Transport and heat flux of the Florida current at 27°N derived from cross-stream voltages and profiling data: theory and observations. Philosophical Transactions of the Royal Society, London A 338:169–236

Latif M, Roeckner E, Botzet M, Esch M, Haak H, Jungclaus J, Legutke S, Marsland S, Mikolajewicz U, Mitchell J (2004) Reconstructing, monitoring and predicting multidecadal-scale changes in the North Atlantic thermohaline circulation with sea surface temperature. Journal of Climate 17:1605–1614

Lee T, Marotzke J (1997) Inferring meridional mass and heat transports of the Indian Ocean by fitting a general circulation model to climatological data. Journal of Geophysical Research 102 (C5):10,585–10,602

Lempert R (2002) A new decision sciences for complex systems. Proceedings of the National Academy of Sciences of the United States of America 99:7309–7313

Longworth HR, Bryden HL, Duncan LM (2005) Historical estimates of Atlantic meridional overturning circulation. Second RAPID Annual Science Meeting and Workshops; http://www.soc.soton.ac.uk/rapid/sci/AnnualMeeting2005.php

Macdonald AM (1998) The global ocean circulation: a hydrographic estimate and regional analysis. Progress in Oceanography 41:281–382

Manabe S, Stouffer RJ (1994) Multiple-century response of a coupled ocean-atmosphere model to an increase of atmospheric carbon dioxide. Journal of Climate 7:5–23

Marotzke J (1997) Boundary mixing and the dynamics of three-dimensional thermohaline circulations. Journal of Physical Oceanography 27:1713–1728

Marotzke J (2000) Abrupt climate change and thermohaline circulation: mechanisms and predictability. Proceedings of the National Academy of Sciences of the United States of America 97:1347–1350

Marotzke J, Cunningham SA, Bryden HL (2002) Monitoring the Atlantic meridional overturning circulation at 26.5°N. Proposal Accepted by the Natural Environment Research Council (UK), Available at: http://www.noc.soton.ac.uk/rapidmoc/

Marotzke J, Giering R, Zhang KQ, Stammer D, Hill C, Lee T (1999) Construction of the adjoint MIT ocean general circulation model and application to Atlantic heat transport sensitivity. Journal of Geophysical Research 104:29,529–29,547

Marotzke J, Klinger BA (2000) The dynamics of equatorially asymmetric thermohaline circulations. Journal of Physical Oceanography 30:955–970

Marsh R, de Cuevas BA, Coward AC, Bryden HL, Alvarez M (2005) Thermohaline circulation at three key section in the North Atlantic over 1985–2002. Geophysical Research Letters 32, doi:10.1029/2004GL022281

Marsland SJ, Haak H, Jungclaus JH, Latif M, Röske F (2003) The Max-Planck-Institute global ocean/sea ice model with orthogonal curvilinear coordinates. Ocean Modelling 5:91–127

McManus JF, Francois R, Gheradi J, Keigwin LD, Brown-Leger S (2004) Collapse and rapid resumption of Atlantic meridional circulation linked to deglacial climate changes. Nature 428:834–837

Mikolajewicz U, Voss R (2000) The role of individual air-sea flux components in CO_2-induced changes of the ocean's circulation and climate. Climate Dynamics 16:627–642

Nakicenovic N, Swart R (2000) Special report on emission scenarios. Technical report, Intergovernmental Panel on Climate Change (IPCC)

National Research Council (2002) Abrupt climate change: inevitable surprises. Alley RB, Marotzke J, Nordhaus WD, Overpeck JT, Peteet DM, Pielke Jr. RA, Pierrehumbert RT, Rhines PB, Stocker TF, Talley LD, Wallace JM, National Academy Press, Washington, D.C

Nordhaus W, Popp D (1997) What is the value of scientific knowledge? An application to global warming using the PRICE model. Energy Journal 1 (18):1–45

Peck SC, Teisberg TJ (1996) Uncertainty and the values of information with stochastic losses from global warming. Risk Analysis 16(2):227–235

Roeckner E, Bäuml G, Bonaventura L, Brokopf R, Esch M, Giorgetta M, Hagemann S, Kirchner I, Kornblueh L, Manzinie E, Rhodin A, Schlese U, Schulzweida U, Tompkins A (2003) The atmospheric general circulation model ECHAM5, part I: model description. Technical Report 349, Max Planck Institute for Meteorology

Santer BD, Mikolajewicz U, Brüggemann W, Cubasch U, Hasselmann K, Höck H, Maier-Reimer E, Wigley TL (1995) Ocean variability and its influence on the detectability of greenhouse warming signals. Journal of Geophysical Research 100 (C6):10693–10725

Schiermeier Q (2004) Gulf Stream probed for early warnings of system failure. Nature 427:769

Stammer D, Wunsch C, Giering R, Eckert C, Heimbach P, Marotzke J, Adcroft A, Hill CN, Marshall J (2003) Volume, heat and freshwater transports of the global ocean circulation 1993–2000, estimated from a general circulation model constrained by World Ocean Circulation Experiment (WOCE) data. Journal of Geophysical Research 108(C1):3007–3030

Stocker TF, Schmittner A (1997) Influence of CO_2 emission rates on the stability of the thermohaline circulation. Nature 388:862–865

Talley L (2003) Shallow, intermediate, and deep overturning components of the global heat budget. Journal of Physical Oceanography 33:530–560

Thorpe RB, Gregory JM, Johns TC, Wood RA, Mitchell JFB (2001) Mechanisms determining the Atlantic thermohaline circulation response to greenhouse gas forcing in a non-flux-adjusted coupled climate model. Journal of Climate 14:3102–3116

Trenberth KE, Solomon A (1994) The global heat balance: heat transport in the atmosphere and ocean. Climate Dynamics 10(3):107–134

Vellinga M, Wood RA (2002) Global climatic impacts of a collapse of the Atlantic thermohaline circulation. Climatic Change 54:251–267

Vellinga M, Wood RA (2004) Timely detection of anthropogenic change in the Atlantic meridional overturning circulation. Geophysical Research Letters 31:L14203, doi: 10.1029/2004GL020306

Wunsch C, Heimbach P (2006) Estimated decadal changes in the North Atlantic meridional overturning circulation and heat flux 1993–2004. Journal of Physical Oceanography, in the press

Yohe G (1991) Uncertainty, climate change and the economic value of information – an economic methodology for evaluating the timing of relative efficacy of alternative response to climate change with application to protecting developed property from greenhouse induced sea-level rise. Policy Sciences 24(3):245–269

Yohe G (1996) Exercises in hedging against extreme consequences of global change and the expected value of information. Global Environmental Change 6:87–101